ChemSusChem

Supporting Information

Towards Solar Factories: Prospects of Solar-to-Chemical Energy Conversion using Colloidal Semiconductor Photosynthetic Systems

Amedeo Agosti,*[a, b] Mirco Natali,[c, d] Lilac Amirav,[b] and Giacomo Bergamini*[a]

Calculation of Threshold Wavelength for Decoupled Photosynthetic Reactions

Decoupled photosynthetic redox reactions present different thermodynamic requirements compared to the overall water splitting reaction. Starting from the definition of the reductive half-reaction, i.e. protons reduction,

$$2H^+ \xrightarrow{2e^-} H_2$$

it is possible to consider a general oxidation of a quencher molecule (Q) as follows:

$$Q \xrightarrow{h^+} Q^+$$

For the case of photochemical processes, the Gibbs free energy of the overall reaction (ΔG_{redox}, with $\Delta G_{redox} = \mu_{redox} \cdot n$) is provided by light absorption. As discussed in the main text, Bolton was the first to explicitly calculate the threshold wavelength fulfilling such thermodynamic requirements[1]:

$$\lambda_{thr} = \frac{hc}{\Delta G_{redox}/n_{PS} + E_{loss}} \qquad [\,m\,] \qquad (1)$$

In order to determine this quantity, it is necessary to calculate E_{loss}, defined as follows:

$$E_{loss} = E_g - E_{redox} \qquad [\,J\,] \qquad (2)$$

where E_{redox} is the net energy available for storage, as schematically pictured in Fig. S1. Clearly, the minimum condition for the photochemical reaction to take place requires $E_{redox} \geq \Delta G_{redox}$.

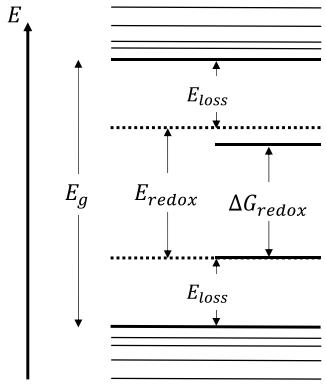

Figure S1. Schematic illustration of E_g, E_{redox}, E_{loss} and ΔG_{redox}

The quantity E_{redox} was first introduced by Ross and Hsiao, who analysed the limit of solar energy conversion using a chemical potential model[2]. In their lucid treatment it is evidenced that not only energy, but also the rate of power extraction should be maximised in real-world devices. In electrical terms, this is the equivalent of the maximum power point operation mode for solar cells. In light of this, the author expressed the net energy available for storage as follows:

$$E_{redox} = E_{max} - k_B T \, ln\left(\frac{E_{max}}{k_B T}\right) \qquad [J] \qquad (3)$$

where k_B is the Boltzmann constant ($[J\,K^{-1}]$), T ($[K]$) the photosynthetic unit temperature and E_{max} ($[J]$) the maximum energy available for photochemical storage under irradiation. Maximum energy is achieved in the ideal limit where no chemical work is extracted from the system: in this scenario the total photon emission rate equals the excitation rate, yielding

$$E_{max} = k_B T ln\left(\frac{J_S + J_{BB}}{J_{BB}}\right) \qquad [J] \qquad (4)$$

with

$$J_S = \int_0^{\lambda_g} I_s(\lambda) d\lambda \qquad [s^{-1}m^{-2}nm^{1}] \qquad (5)$$

$$J_{BB} = \int_0^{\lambda_g} I_{BB}(\lambda) d\lambda \qquad [s^{-1}m^{-2}nm^{-1}] \qquad (6)$$

in which J_S is the absorbed photon flux and J_{BB} the photon flux emitted by a blackbody at temperature T. Both J_S and J_{BB} are obtained by evaluating the incident photon flux (I_s) and blackbody photon flux (I_{BB}) over the wavelength range $\lambda \leq \lambda_g$, respectively. To this extent, the photosynthetic unit is assumed to as a perfect absorber, where photons with energy equal or above the band-gap threshold are absorbed with unit quantum efficiency.

Finally, the values for ΔG_{redox} are obtained using the Nernst equation and tabulated values for the oxidation and reduction half-reactions. In this work it was chosen to analyse recent demonstrations of solar-to-chemical (STC) energy conversion experiments, namely the simultaneous reduction of H^+ and oxidation of benzylamine($BnNH_2$)[3] and 4-methylbenzyl alcohol($4-MBA$)[4]. According to the experimental condition used in the respective studies, the following values for the electrochemical potential were used[5,6]:

$$V_{H^+/BnNH_2}(pH = 7) = V_{red} - V_{ox} = -0.414 - (1.324) = -1.738\ V$$

$$V_{H^+/4-MBA}(pH = 4.5) = V_{red} - V_{ox} = -0.266 - (1.849) = -2.115\ V$$

Overall, in order to calculate λ_{thr}, a recursive method should be used to evaluate equations 6 to 1, owing to the fact that all the quantities involved are wavelength dependent. Table 1 summarises the values obtained when proton reduction is coupled to water (H^+/OH^-), benzylamine ($H^+/BnNH_2$) and 4-methoxybenzyl-alcohol oxidation (H^+/4-MBA).

Red/Ox species	ΔG_{redox} [eV]	λ_{ideal} [nm]	$E_{loss}(\lambda_{max})$ [meV]	λ_{thr} [nm]
H^+/OH^-	1.23	1010	375	788
$H^+/BnNH_2$	1.74	713	420	583
$H^+/4-MBA$	2.12	586	457	489

Table 1. Thermodynamic requirements for different decoupled photosynthetic red-ox reactions.

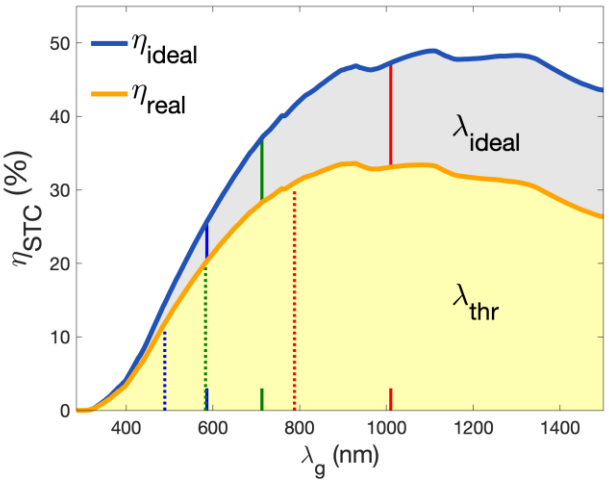

Figure S2. Threshold wavelengths for the ideal (λ_{ideal}, solid lines) and real (λ_{thr}, dashed lines) STC conversion limits

Analysis of Photoluminescence Quenching via Absorption Spectroscopy

Comprehensive analysis of photoluminescence quenching necessitates corroboration of the data obtained with emission spectra with absorption optical spectroscopy. With this technique it is possible to identify the presence of spectral overlap between the absorption spectrum of the photosynthetic unit and the emission profile of the quencher. As shown in Figure S3, absence of spectral superposition excludes Förster and Dexter energy-transfer mechanisms, that can compete with photo-induced electron transfer in determining photoluminescence quenching.

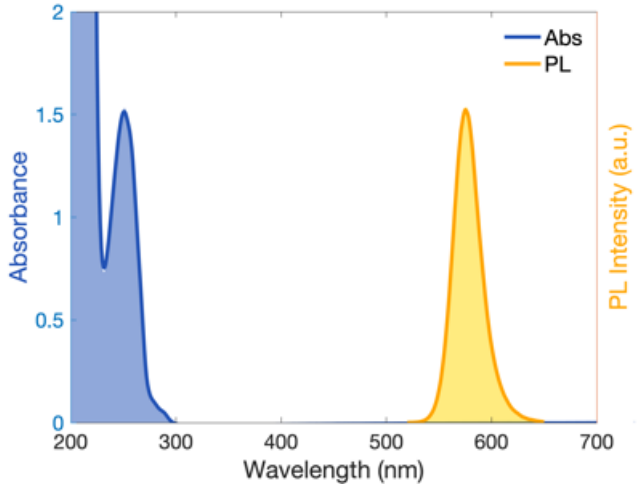

Figure S3. Absorption (blue curve) and emission (orange curve) spectra of distinct diluted solutions (H_2O:CH_3CN, 60:40) of benzylamine and CdSe@CdS seeded nanorods.

Estimation of Fraction of Absorbed Solar Photon Flux

Figure S4 presents absorption spectra for different concentration of Pt-tipped CdSe@CdS colloidal seeded nanorods (Pt-SR)[7]. Liquid solutions of such hybrid nanostructures present a non-negligible scattering caused by Pt quantum dots. In order properly estimate the absorbed photon flux, this contribution was isolated via the application of the Rayleigh scattering model:

$$A = log\left(\frac{I_0}{I_0 - I_{scatt}}\right) + A_0 = log\left(\frac{1}{1 - k\lambda^{-4}}\right) + A_0 \qquad (7)$$

where I_0 is the incoming light, I_{scatt} the scattered fraction (scaling with the fourth power of incident wavelength) and k a constant of proportionality.

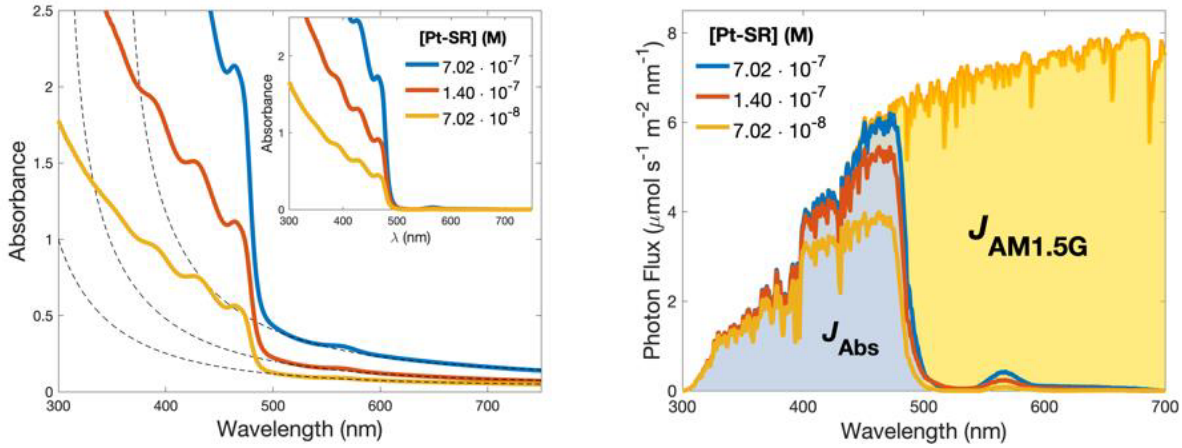

Figure S4. (A) Absorption spectra of different concentrations ($c = 7.02 \cdot 10^{-8} \div 7.02 \cdot 10^{-7}\, M$) of Pt-tipped CdSe@CdS Seeded nanoRods (Pt-SR), showing varying fraction of light absorbed at the first exciton peak: 64% (yellow curve), 88% (red curve), 99% (blue curve). Inset: same curves after removal of the scattering contribution (black dashed curve) from Pt quantum, fitted via Rayleigh model. (B) Reference AM1.5G photon flux ($J_{AM1.5G}$, yellow curve) and fraction of absorbed photon flux(J_{Abs}, shaded light-blue areas) absorbed by the different Pt-SR concentrations. Photon fluxes are expressed in mole of photons, or einstein.

The precise determination of absorption profiles is particularly relevant for the estimation of photochemical quantum efficiency for reaction promoted by polychromatic sources. For the case of simulated solar sunlight, the absorbed photon flux (J_{Abs}) can be calculated according to the following formula:

$$J_{Abs} = A \int \frac{J_{AM1.5G}(\lambda)}{E(\lambda)}\, \eta_{abs}(\lambda) d\lambda \qquad [\, s^{-1}\,] \tag{8}$$

where A is the irradiated area ([m^2]), $J_{AM1.5G}$ the AM1.5G solar spectrum ([$s^{-1}\, m^{-2}\, nm^1$]), E the photon energy and η_{abs} the fraction of light absorbed by the photosynthetic unit. The latter quantity is determined by the Beer-Lambert-Bouguer law for liquid solutions:

$$\eta_{abs,\lambda} = 1 - 10^{-A(\lambda)} = 1 - 10^{-\varepsilon(\lambda) c l} \tag{9}$$

in which A is the absorbance determined after removing the scattering contribution, ε ([$M^{-1}cm^{-1}$]) the molar absorption coefficient, c ([M]) the semiconductor concentration and l (cm]) the optical path length.

[Pt-SR] [M]	$A(\lambda = 455\ nm)$ [ ]	η_{abs} [%]	k [nm^4]	J_{Abs} [$s^{-1}\ m^2$]
$\mathbf{7.02 \cdot 10^{-8}}$	0.5	68.4	$1.70 \cdot 10^{10}$	$3.27 \cdot 10^{20}$
$\mathbf{1.40 \cdot 10^{-7}}$	1	90	$9.00 \cdot 10^{9}$	$4.03 \cdot 10^{20}$
$\mathbf{7.02 \cdot 10^{-7}}$	2	99	$5.01 \cdot 10^{9}$	$4.33 \cdot 10^{20}$

Table 2. Computation of the absorbed photon fluxes for varying [Pt-SR]

STC Efficiency

Figure 2B shows the results obtained for a STC photosynthetic experiment, where Pt-CdSe@CdS seeded nanorods are used for the decoupled H^+ reduction and benzylamine oxidation, performed in a 60:40 water:acetonitrile mixture under AM1.5G irradiation (1 Sun).

For the case of $[BnNH_2] = 50\ mM$, STC efficiency is estimated using equation 3 and 1 in the main text:

(3) $$\mu_{redox} = -z \cdot \mathcal{F} \cdot V = -z \cdot \mathcal{F} \cdot (V_{red} - V_{ox})$$

$$\mu_{H^+/BnNH_2} = -2 \cdot 96{,}485 \left[\frac{kJ}{V \cdot mol}\right] \cdot \{-0.414 - (1.324)\}[V] = \mathbf{335.4}\ [\boldsymbol{kJ\ mol^{-1}}]$$

(1) $$\eta_{STC,max}\ (\%) = \frac{I_{mol,max} \cdot \mu_{redox}}{P_{AM1.5G} \cdot A} \cdot 100\%$$

$$\eta_{STC,max}\ (\%) = \frac{1.28 \cdot 10^{-8}[mol\ s^{-1}] \cdot 3.354 \cdot 10^{5}[J\ mol^{-1}]}{0.1\ [W\ cm^{-2}] \cdot 3.5\ [cm^2]} \cdot 100\% = \mathbf{1.22}\%$$

REFERENCES

1. Bolton, J. R., Haught, A. F. & Ross, R. T. Photochemical Energy Storage: An Analysis of Limits. in *Photochemical Conversion and Storage of Solar Energy* 297–346 (1981).

2. Ross, R. T. & Hsiao, T.-L. Limits on the yield of photochemical solar energy conversion. *J. Appl. Phys.* **48**, 4783–4785 (1977).

3. Agosti, A., Nakibli, Y., Amirav, L. & Bergamini, G. Photosynthetic H_2 generation and organic transformations with CdSe@CdS-Pt nanorods for highly efficient solar-to-chemical energy conversion. *Nano Energy* **70**, (2020).

4. Kasap, H. *et al.* Solar-driven reduction of aqueous protons coupled to selective alcohol oxidation with a carbon nitride−molecular Ni catalyst system. *J. Am. Chem. Soc.* **138**, 9183–9192 (2016).

5. Wang, Z. J., Garth, K., Ghasimi, S., Landfester, K. & Zhang, K. A. I. Conjugated Microporous Poly(Benzochalcogenadiazole)s for Photocatalytic Oxidative Coupling of Amines under Visible Light. *ChemSusChem* **8**, 3459–3464 (2015).

6. Yasuda, M., Nakai, T., Kawahito, Y. & Shiragami, T. Micelle-Enhancing Effect on a Flavin-Photosensitized Reaction of Benzyl. *Bull. Chem. Soc. Jpn.* **76**, 601–605 (2003).

7. Kalisman, P., Nakibli, Y. & Amirav, L. Perfect photon-to-hydrogen conversion efficiency. *Nano Lett.* **16**, 1776–1781 (2016).